Weakly bound $s_{1/2}$ neutrons in the many-body pair correlation of neutron drip line nuclei

Ikuko Hamamoto[1,2,3] and Ben R. Mottelson[2,4]
[1]Division of Mathematical Physics, Lund Institute of Technology at the University of Lund, Lund, Sweden
[2]The Niels Bohr Institute, Blegdamsvej 17, Copenhagen Ø, DK-2100, Denmark
[3]Radiation Laboratory, RIKEN, Wako-shi, Saitama 351-0198, Japan
[4]NORDITA, Blegdamsvej 17, Copenhagen Ø, DK-2100, Denmark
(Received 15 December 2003; published 2 June 2004)

With a simplified model in the Hartree-Fock-Bogoliubov (HFB) approximation, the behavior of weakly bound $s_{1/2}$ neutrons in the many-body pair correlation is studied by solving the HFB equation in coordinate space with the correct asymptotic boundary conditions. It is shown that in one-neutron pickup reactions on the even-even neutron-drip-line nuclei, which contain loosely bound $s_{1/2}$ neutrons, the strength of the $s_{1/2}$ neutron can appear both at a discrete state and in the low-energy continuum spectra, with comparable strength. When there is no weakly bound discrete state, the continuum spectra may exhibit a sharp peak just above $E_x=|\lambda|$, which originates from the resonantlike behavior of the upper component of the HFB radial wave function, $u_{s1/2}(E_{qp},r)$. This resonantlike behavior may be directly observed as an s-wave resonance close to $E_x=|\lambda|$ in neutron-scattering experiments on those nuclei. It is also shown that a very large root-mean-square radius of loosely bound $s_{1/2}$ neutrons may appear also in the presence of many-body pair correlation, since the effective pair gap in weakly bound neutron orbits with low ℓ values is much reduced.

DOI: 10.1103/PhysRevC.69.064302 PACS number(s): 21.60.Ev, 21.10.Pc, 21.60.Jz

I. INTRODUCTION

The study of nuclear structure for nuclei close to the drip lines is currently one of the most active and interesting fields experimentally as well as theoretically. A special feature of the weakly bound neutron systems is the importance of coupling to the nearby continuum of unbound states; this phenomenon is not present for weakly bound proton systems because of the Coulomb barrier. Since weakly bound neutrons with small orbital angular momentum ℓ have an appreciable probability to be outside of the core nucleus, those neutrons are insensitive to the strength (radius and/or depth) of the potential provided by the well-bound nucleons in the system. In particular, the behavior of $s_{1/2}$ neutrons is an extreme case since the centrifugal barrier is absent for the $\ell=0$ orbit. This difference in the properties of small ℓ neutrons from those of weakly bound large ℓ neutrons, for which the wave functions stay mostly inside the potential, is known to lead to drastic effects on the shell structure in some neutron drip line nuclei. In medium-heavy nuclei the occupancy of weakly bound $s_{1/2}$ neutron orbits will never make a significant contribution to the one-body potential and the many-body pair correlation, since those $s_{1/2}$ particles are weakly coupled to the core, in addition to the very small number of particles which can occupy the $s_{1/2}$ orbits. Nevertheless, the nuclear matter density at large radii can be decisively influenced by such weakly bound $s_{1/2}$ neutrons.

In Ref. [1] the Hartree-Fock-Bogoliubov (HFB) equation in a simplified model was solved in coordinate space with the correct asymptotic boundary conditions [2–4], and the pair correlation in nuclei close to the neutron drip line was studied. It was shown that the occupation probability of the lower-ℓ orbits of the Hartree-Fock (HF) potential decreases considerably when the binding energy of the HF one-particle level becomes small, and those orbits soon become almost unavailable for the pair correlation of the many-body system. In the present paper we employ the same model as used in Ref. [1] and study in detail the properties related to the weakly bound $s_{1/2}$ neutron orbits.

In Sec. II our model is briefly described, while numerical results and discussions are given in Sec. III. Conclusions are drawn in Sec. IV.

II. MODEL

In the present section only a brief summary of our model is given, since the model is exactly the same as that used in Ref. [1]. We consider the time-reversal invariant and spherically symmetric system with monopole pairing correlation. Considering the coupling of the one-quasiparticle neutron with ℓ and j to the HF field, $V(r)$ and $V_{so}(r)$, and the pairing field $\Delta(r)$, both of which are given by the core nucleus, our HFB equation is reduced to the two-channel coupled equation

$$\begin{aligned}
&\left\{\frac{d^2}{dr^2}-\frac{\ell(\ell+1)}{r^2}+\frac{2m}{\hbar^2}[\lambda+E_{qp}-V(r)-V_{so}(r)]\right\}\\
&\times u_{\ell j}-\frac{2m}{\hbar^2}\Delta(r)v_{\ell j}=0,\\
&\left\{\frac{d^2}{dr^2}-\frac{\ell(\ell+1)}{r^2}+\frac{2m}{\hbar^2}[\lambda-E_{qp}-V(r)-V_{so}(r)]\right\}\\
&\times v_{\ell j}+\frac{2m}{\hbar^2}\Delta(r)u_{\ell j}=0,
\end{aligned} \tag{1}$$

where $u_{\ell j}$ and $v_{\ell j}$ express the upper and lower components of the radial wave functions in the HFB approximation, respectively. We take positive quasiparticle energies $E_{qp}>0$ and consider bound states $\lambda<0$. Then, $(\lambda-E_{qp})$ is always negative, while $(\lambda+E_{qp})$ can be either negative or positive. The asymptotic boundary conditions and the normalization of the wave functions are described in Refs. [1,2,4].

Then, for simplicity, we replace the HF potential by the Woods-Saxon potential together with the spin-orbit potential, of which the parameters are the standard ones used in β stable nuclei [1,5]. For the given radius $R=r_0A^{1/3}$ with $r_0=1.27$ fm, the diffuseness $a=0.67$ fm and the strength of spin-orbit potential, we vary the potential strength by changing the depth of the Woods-Saxon potential V_{WS} so that the corresponding (HF) single-particle energy ε_{WS} is varied. We show numerical results with the volume-type pairing,

$$\Delta(r) \propto f(r), \tag{2}$$

where

$$f(r) = \frac{1}{1+\exp\left(\dfrac{r-R}{a}\right)} \tag{3}$$

since the surface-type pairing leads to essentially the same physics conclusion. The averaged strength of the pair field defined by

$$\bar{\Delta} \equiv \frac{\int_0^\infty r^2 dr \Delta(r) f(r)}{\int_0^\infty r^2 dr\ f(r)} \tag{4}$$

is an input of numerical calculations expressing the strength of the pair field.

It should be emphasized that both the one-body potential $V(r)$ and the pair field $\Delta(r)$ come almost exclusively from the well-bound or (weakly bound, but) high-ℓ particles, and not from loosely bound $s_{1/2}$ neutrons. Thus in our present work we study the behavior of weakly bound $s_{1/2}$ neutrons in the many-body pair correlation for given $V(r)$ and $\Delta(r)$.

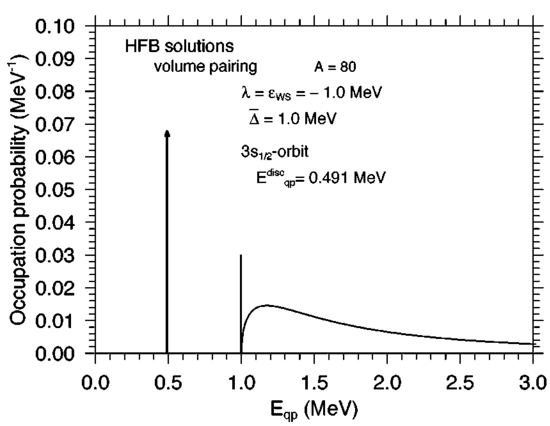

FIG. 1. Occupation probability (7) of HFB continuum solutions for the $3s_{1/2}$ orbit and $\lambda=\varepsilon_{WS}=-1.0$ MeV as a function of quasiparticle energy E_{qp}. The quasiparticle energy of the discrete solution of the HFB equation, $E_{qp}^{disc}=0.491$ MeV, is indicated by the thick arrow. The one-particle energy eigenvalue for the Woods-Saxon potential is expressed by ϵ_{WS}. The vertical thin line shows the position of $|\lambda|$. See the text for details.

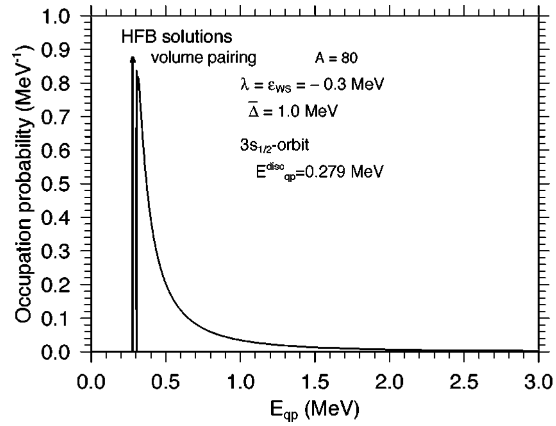

FIG. 2. Occupation probability (7) of HFB continuum solutions for the $3s_{1/2}$ orbit and $\lambda=\varepsilon_{WS}=-0.3$ MeV as a function of quasiparticle energy. The quasiparticle energy of the discrete solution of the HFB equation, $E_{qp}^{disc}=0.279$ MeV, is indicated by the thick arrow. The vertical thin line shows the position of $|\lambda|$. Note that the scale of the y axis is one order of magnitude different from that of Fig. 1. See the caption to Fig. 1.

III. NUMERICAL RESULTS AND DISCUSSIONS

In numerical calculations we take $\bar{\Delta}=1.0$ MeV and vary ε_{WS} keeping the condition $\lambda=\varepsilon_{WS}$ so that the particular single-particle level with ε_{WS} should be considerably occupied, hopefully by about 50%. As $\lambda(<0)$ increases to zero, we simulate neutron drip line nuclei, in which the one-particle level is placed on the Fermi level.

Since in Ref. [1] some properties of HFB solutions of the $3s_{1/2}$ orbit are already shown taking the $A=80$ system, in the present study we consider the same system. Indeed, the $3s_{1/2}$ orbit is the first $s_{1/2}$ orbit that can occur near the Fermi level of neutron drip line nuclei, for which the many-body pair correlation may play a role. In Figs. 1–4 the calculated occupation probability is shown for the cases of $\lambda=\varepsilon_{WS}=-1.0, -0.3, -0.2$, and -0.1 MeV, respectively. In the first two

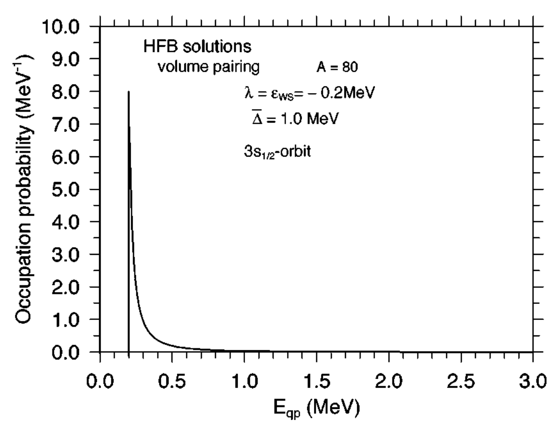

FIG. 3. Occupation probability (7) of HFB continuum solutions for the $3s_{1/2}$ orbit and $\lambda=\varepsilon_{WS}=-0.2$ MeV as a function of quasiparticle energy. No discrete solution of the HFB equation is obtained for the present parameters. The vertical thin line shows the position of $|\lambda|$. Note that the scale of the y axis is one order of magnitude different from that of Fig. 2. See the caption to Fig. 1.

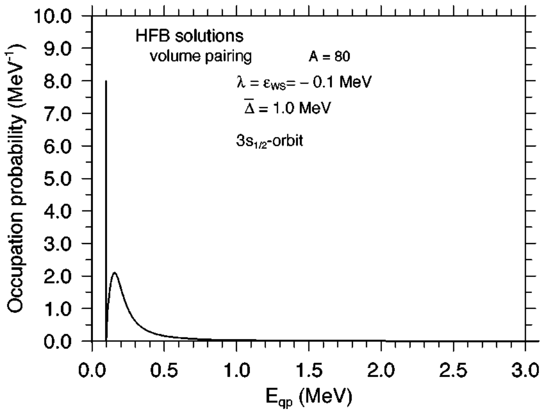

FIG. 4. Occupation probability (7) of HFB continuum solutions for the $3s_{1/2}$ orbit and $\lambda=\varepsilon_{WS}=-0.1$ MeV as a function of quasiparticle energy. No discrete solution of the HFB equation is obtained for the present parameters. The vertical thin line shows the position of $|\lambda|$. Note that the scale of the y axis is one order of magnitude different from that of Fig. 2. See the caption to Fig. 1.

cases a discrete solution is obtained at $E_{qp}^{disc}=0.491$ and 0.279 MeV, respectively, while in the latter two cases no discrete solutions are found. The presence of the discrete solution with $E_{qp}^{disc}=0.279$ MeV clearly shows that the effective pair gap for the $3s_{1/2}$ orbit at $\lambda=\varepsilon_{WS}=-0.3$ MeV is less than 0.279 MeV, which is much smaller than the averaged value $\bar{\Delta}=1$ MeV. It is noted that the effective pair gap for large ℓ orbits, for example, the $1g$ orbit, is always larger than the value of $\bar{\Delta}$ [1].

The occupation probability for the discrete solution is

$$\int_0^\infty |v_{\ell j}(E_{qp}^{disc},r)|^2 dr, \quad \text{where} \quad (\lambda + E_{qp}^{disc}) < 0, \tag{5}$$

for which the normalization of the wave functions is written as

$$\int_0^\infty [|u_{\ell j}(E_{qp},r)|^2 + |v_{\ell j}(E_{qp},r)|^2] dr = 1, \tag{6}$$

while that for the continuum solution, which is plotted in Figs. 1–4, is

$$\int_0^\infty |v_{\ell j}(E_{qp},r)|^2 dr, \quad \text{where} \quad (\lambda + E_{qp}) > 0, \tag{7}$$

which represents the occupation number probability density per unit energy interval [2]. Since the dimensions of the two expressions (5) and (7) are different due to the difference in the normalization of radial wave functions, in Figs. 1 and 2 the discrete quasiparticle energy is indicated by the thick arrow, while in the cases of Figs. 3 and 4 there is no such discrete quasiparticle solution. In Table I the $3s_{1/2}$ occupation probability of the continuum solution integrated over the relevant energy region,

TABLE I. Properties of $3s_{1/2}$ neutron orbits: Energy of discrete solution (if it exists), occupation probabilities of discrete and continuum solutions, and the expectation values of radius squared as a function of $\varepsilon_{WS}=\lambda$. No discrete quasiparticle solution was found for the parameters $\varepsilon_{WS}=\lambda$, if the value of E_{qp}^{disc} is not written. $\bar{\Delta}=1$ MeV is used. See the text for the definition of various quantities.

$\varepsilon_{WS}=\lambda$ (MeV)	E_{qp}^{disc} (MeV)	v_{disc}^2	v_{cont}^2	$\langle r^2\rangle_{disc}$ (fm^2)	$\langle r^2\rangle_{cont}$ (fm^2)	$\langle r^2\rangle_{total}$ (fm^2)	$\langle r^2\rangle_{WS}$ (fm^2)
−10	0.957	0.476		22.7		22.7	23.3
−1	0.491	0.433	0.021	46.7	34.6	46.1	55.2
−0.5	0.367	0.380	0.059	59.4	45.9	57.5	77.4
−0.3	0.279	0.274	0.157	72.2	59.9	67.6	102.4
−0.2			0.418		76.9	76.9	130.8
−0.1			0.399		94.9	94.9	205.9

$$v_{cont}^2 \equiv \int_{|\lambda|}^{10} dE_{qp} \int_0^{70} dr |v_{s1/2}(E_{qp},r)|^2, \tag{8}$$

and that of the discrete solution,

$$v_{disc}^2 \equiv \int_0^{70} dr |v_{s1/2}(E_{qp}^{disc},r)|^2, \tag{9}$$

are tabulated. When v_{cont}^2 is calculated, the quasiparticle energy is integrated until 10 MeV while the radial integration is carried out until 70 fm. For $\lambda=\varepsilon_{WS}<-1$ MeV the amount of v_{cont}^2 is negligibly small, while for $\lambda=\varepsilon_{WS}>-0.221$ MeV the value of v_{disc}^2 is zero, since no discrete solution exists. It is seen that varying $\lambda=\varepsilon_{WS}$ from −1 to −0.2 MeV the $3s_{1/2}$ occupation probability moves smoothly from the discrete to continuum solutions. Furthermore, the peak energy of the quantity (7) approaches $E_{qp}=|\lambda|$ as $\lambda=\varepsilon_{WS}(<0)$ increases up till about −0.22 MeV, while it goes away from $E_{qp}=|\lambda|$ when $\lambda=\varepsilon_{WS}$ increases further. And, the peak lies at $E_{qp}\approx|\lambda|$ at the value of $\lambda=\varepsilon_{WS}\approx-0.22$ MeV after which the discrete solution disappears; see Fig. 3 and note that the scale of the y axis in Figs. 3 and 4 is different from those of Figs. 1 and 2 by two and one orders of magnitude, respectively.

The result presented in Figs. 1–4 suggests that if one performs one-neutron pickup reactions on those even-even neutron-drip-line nuclei, which contain loosely bound $s_{1/2}$ neutrons around the Fermi level, the strength of the $s_{1/2}$ neutron can appear both at a discrete state and in the continuum spectra, with comparable magnitudes. Then, the occupation probability of the $s_{1/2}$ orbit in the ground state of the target nucleus must be estimated by summing up those two kinds of strength. In the case that the population of the discrete state is absent, the continuum spectra may exhibit a sharp peak just above $E_x=|\lambda|$, which originates from the resonant-like behavior of the upper radial wave function, $u_{s1/2}(E_{qp},r)$.

The relation between the phase shifts of the upper component of the radial wave function $u_{\ell j}(E_{qp},r)$ in the presence and absence of the pairing potential $\Delta(r)$ is discussed in Refs. [2,4] in the case of the quasiparticle resonant solutions induced by the bound single-particle states. For $\ell=0$ neu-

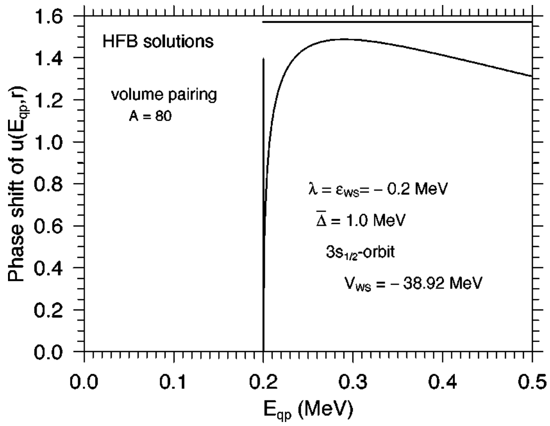

FIG. 5. Calculated phase shift of the upper component of the radial wave function $u_{3s1/2}(E_{qp},r)$ for the parameters of Fig. 3. The vertical thin line shows the position of $|\lambda|$, while the horizontal thin line denotes the value of $\pi/2$. The used depth of the Woods-Saxon potential is denoted by V_{WS}.

trons the phase shift (δ) of the radial wave functions does not increase through $\pi/2$ as energy increases, if the pair potential $\Delta(r)$ is absent. In contrast, in the presence of the pair potential the phase shift of $u_{s1/2}(E_{qp},r)$ may increase through $\pi/2$ as energy increases, but the energy at $\delta=\pi/2$ does not in general correspond to a resonance behavior of $u_{s1/2}(E_{qp},r)$. In Fig. 5 we show the calculated phase shift of $u_{s1/2}(E_{qp},r)$ for the parameters of Fig. 3. We observe a sharp increase of the phase shift, or a large positive value of the derivative $d\delta/dE_{qp}$, slightly above $E_{qp}=|\lambda|=0.2$ MeV, which leads to the sharp peak of the occupation probability in Fig. 3 around the same energy. For reference, the calculated phase shift for the parameters of Fig. 2 is shown in Fig. 6, which exhibits a large negative value of the derivative $d\delta/dE_{qp}$ at $E_{qp}\approx|\lambda|=0.3$ MeV. For the present set of parameters the value of $d\delta/dE_{qp}$ slightly above $E_{qp}=|\lambda|$ changes from $-\infty$ to $+\infty$ when the value of $\varepsilon_{WS}=\lambda$ increases through -0.221 MeV. And, at this energy the discrete solution [namely the bound-state solution of $u_{s1/2}(E_{qp},r)$] disappears.

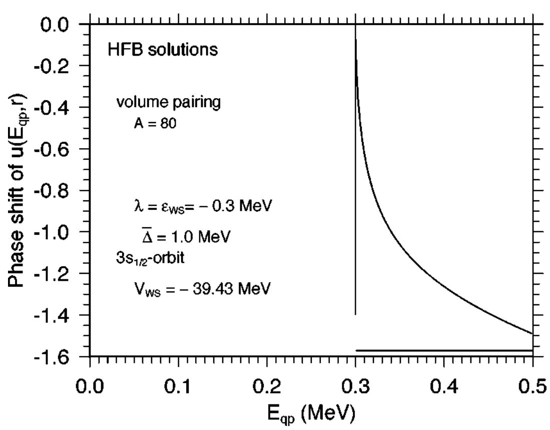

FIG. 6. Calculated phase shift of the upper component of the radial wave function $u_{3s1/2}(E_{qp},r)$ for the parameters of Fig. 2. The vertical thin line shows the position of $|\lambda|$, while the horizontal thin line denotes the value of $-\pi/2$.

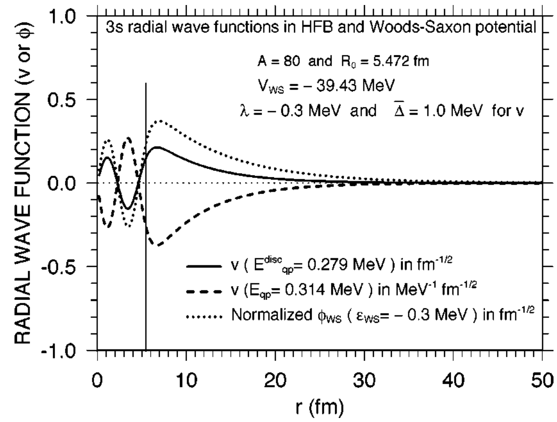

FIG. 7. Comparison between the shapes of three $s_{1/2}$ radial wave functions for the parameters of Fig. 2; the normalized $3s_{1/2}$ eigenfunction of the Woods-Saxon potential $\phi_{WS}(r)$, the discrete solution of the HFB equation $v(E_{qp}^{disc}=0.279\text{ MeV},r)$, and the continuum solution of the HFB equation $v(E_{qp}=0.314\text{ MeV},r)$ where 0.314 MeV is the peak energy of the continuum occupation probability shown in Fig. 2. All three wave functions are bound-state wave functions, however, only the shapes of those wave functions should be compared, since the continuum solution $v(E_{qp}=0.314\text{ MeV},r)$ shown by the dashed curve has a different dimension from the other two.

The sharp resonantlike behavior of $u_{s1/2}(E_{qp},r)$ obtained for $\varepsilon_{WS}=\lambda\approx-0.2$ MeV suggests that the cross section of the neutron scattering on those even-even nuclei will show the s-wave resonance structure at an energy close to $E_x=|\lambda|$. Neutron s-wave resonances in heavy nuclei at very low energy have been extensively studied since their discovery in 1935 (for example, see p. 176 of Ref. [5]). In those reactions on β stable nuclei the relevant nuclear states are at high excitation energy ($E_x\approx S_n\approx 5-7$ MeV) and the spectroscopic factors of the $s_{1/2}$ state is of the order of 10^{-6}. In contrast, the spectroscopic factor of the present example of s-wave resonance, which may be observed at very low excitation energy $E_x\approx|\lambda|$ (typically, a few hundred keV) for some neutron drip line nuclei, may be of the order of $10^{-1}-10^{-2}$. In the absence of pair field for a given one-body potential such neutron s-wave resonances are expected to occur just before the potential strength becomes strong enough to make an s-wave one-particle bound state. In contrast, in the presence of pair field the s-wave resonance may be observed for neutron drip line nuclei, in which an $s_{1/2}$ level lies around the Fermi level λ ($\approx-$a few hundred keV).

In Fig. 7 the shape of three $s_{1/2}$ radial wave functions are compared taking the same parameters as those used in Fig. 2. The wave function $\phi_{WS}(r)$ of the Woods-Saxon eigenstate with the eigenvalue -0.3 MeV is shown by the dotted curve which are normalized to unity, while the lower radial wave function $v(E_{qp}^{disc}=0.279\text{ MeV},r)$ is denoted by the solid curve. The wave function $v(E_{qp}=0.314\text{ MeV},r)$ is shown by the dashed curve, where 0.314 MeV is the peak energy of the continuum occupation probability exhibited in Fig. 2. Though all three wave functions are bound-state wave functions, we should compare only the shape of those wave functions in Fig. 7, since the wave function denoted by the dashed curve has a dimension different from the other two. It is seen that wave functions expressed by the dashed and solid curves, which are calculated in the presence of pair correlation, extend to the far outside of the radius of the Woods-Saxon potential, because the effective pair gap for the $3s_{1/2}$ orbit with such a small binding energy is very much reduced. In Table I we show the expectation value of r in the discrete solution

$$\langle r^2\rangle_{disc} \equiv \frac{\int_0^{70} r^2 dr |v(E_{qp}^{disc}, r)|^2}{v_{disc}^2}, \tag{10}$$

the one in the continuum solution

$$\langle r^2\rangle_{cont} \equiv \frac{\int_{|\lambda|}^{10} dE \int_0^{70} r^2 dr |v(E,r)|^2}{v_{cont}^2}, \tag{11}$$

the averaged value over the discrete and continuum solutions

$$\langle r^2\rangle_{total} \equiv \frac{\int_0^{70} r^2 dr |v(E_{qp}^{disc}, r)|^2 + \int_{|\lambda|}^{10} dE \int_0^{70} r^2 dr |v(E,r)|^2}{v_{disc}^2 + v_{cont}^2}, \tag{12}$$

and the one in the normalized $3s_{1/2}$ eigenstate with ε_{WS} of the Woods-Saxon potential

$$\langle r^2\rangle_{WS} \equiv \int_0^{70} r^2 dr |\phi_{WS}(r)|^2. \tag{13}$$

It is seen from Table I that even in the presence of the many-body pair correlation the root-mean-square radius of the $3s_{1/2}$ neutron orbit can become very large in the limit of $\lambda = \varepsilon_{WS} \to 0$, due to the considerably reduced effective pair gap for loosely bound $s_{1/2}$ neutrons. Consequently, we expect that so-called halo phenomena (in particular, the presence of an appreciable tail of the ground-state matter density at anomalously large radii, which must come from $s_{1/2}$ neutrons) can be generated in the presence of many-body pair correlations. For a different conclusion concerning this interesting question, see Ref. [6].

In Fig. 8 we plot v_{disc}^2 from Eq. (9), v_{cont}^2 from Eq. (8), and the total occupation probability of the $s_{1/2}$ state,

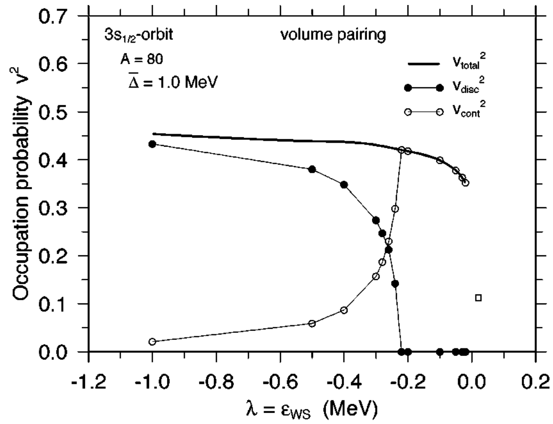

FIG. 8. Occupation probabilities v_{disc}^2, v_{cont}^2, and v_{total}^2 as a function of $\lambda = \varepsilon_{WS}$. The relation $\lambda = \varepsilon_{WS}$ does not hold for the open square plotted at $\varepsilon_{WS} = +0.02$ MeV for v_{total}^2, which was obtained by using $V_{WS} = -36.259$ MeV and $\lambda = -0.02$ MeV. See the text for details.

$$v_{total}^2 = v_{disc}^2 + v_{cont}^2, \tag{14}$$

as a function of $\lambda = \varepsilon_{WS} > -1.0$ MeV. It is remarkable to observe that v_{total}^2 of the $s_{1/2}$ state is only slightly decreasing until $\lambda = \varepsilon_{WS} (< 0)$ approaches within a few tens of keV to the continuum. In order to obtain an indication of an approximate value of v_{total}^2 for $\varepsilon_{WS} \gtrsim 0$, by an open square we denote the value of v_{total}^2 at $\varepsilon_{WS} = +0.02$ MeV. The value was estimated for the depth of the Woods-Saxon potential $V_{WS} = -36.259$ MeV, which was obtained by extrapolating the relation between ε_{WS} and V_{WS} for $\varepsilon_{WS} \lesssim 0$, while we used $\lambda = -0.02$ MeV since λ must be negative in the present discussion. For reference, we obtain $\varepsilon_{WS} = 0$ for $V_{WS} = -36.878$ MeV.

IV. CONCLUSIONS

Using a simplified model in HFB approximation, we have studied the characteristic feature of weakly bound neutrons unique to those in $s_{1/2}$ orbits in neutron drip line nuclei. The effective pair gap of loosely bound $s_{1/2}$ neutrons is much reduced compared with that of neutrons with larger ℓ values. The small pair gap leads to a large root-mean-square radius of those $s_{1/2}$ neutrons lying close to the Fermi level, even in the presence of many-body pair correlation. If one-neutron pickup reactions on those even-even neutron-drip-line nuclei can be performed, the strength of the $s_{1/2}$ neutron may appear both at a discrete state and in the continuum. If the pickup strength of the $s_{1/2}$ neutrons is not observed at a discrete state, the cross section of the neutron scattering on the even-even nuclei can exhibit s-wave resonance structure at the positive energies corresponding to $|\lambda| \approx$ a few hundred keV.

[1] I. Hamamoto and B. R. Mottelson, Phys. Rev. C **68**, 034312 (2003).
[2] A. Bulgac, nucl-th/9907088.
[3] S. T. Belyaev, A. V. Smirnov, S. V. Tolokonnikov, and S. A. Fayans, Sov. J. Nucl. Phys. **45**, 783 (1987).
[4] M. Grasso, N. Sandulescu, Nguyen Van Giai, and R. J. Liotta, Phys. Rev. C **64**, 064321 (2001).
[5] A. Bohr and B. R. Mottelson, *Nuclear Structure* (Benjamin, Reading, MA, 1969), Vol. I.
[6] K. Bennaceur, J. Dobaczewski, and M. Ploszajczak, Phys. Lett. B **496**, 154 (2000).